

Supporting Information

**Computational Screening of High Activity and Selectivity of
CO₂ Reduction via Transition Metal Single-Atom Catalysts
on Triazine-based Graphite Carbon Nitride**

Shuang Ji,^a Yi Li,^{*ab} Yongfan Zhang^{ab} and Wei Lin ^{*ab}

^a State Key Laboratory of Photocatalysis on Energy and Environment, College of Chemistry, Fuzhou University, Fuzhou 350108, P.R. China

^b Fujian Provincial Key Laboratory of Theoretical and Computational Chemistry, Xiamen University, Xiamen, Fujian 361005, China;

* To whom correspondence should be addressed. Email: liy99@fzu.edu.cn; wlin@fzu.edu.cn

Table S1. Calculated thermodynamic quantities of gas-phase molecules, including energy, zero-point energy correction, enthalpic temperature correction, and entropy contribution, respectively.

Species	E / (eV)	ZPE / (eV)	$\int C_p dT$ / (eV)	TS / (eV)
CO ₂	-23.07	0.30	0.10	0.66
CO	-14.78	0.13	0.09	0.69
H ₂	-6.76	0.27	0.09	0.43
HCOOH	-30.24	0.89	0.11	0.84
CH ₃ OH	-30.43	1.36	0.11	0.78
H ₂ O	-14.54	0.56	0.10	0.67
CH ₄	-24.02	1.19	0.10	0.58

Table S2. Formation energy (E_f) and dissolution potential (U_{diss}) of metals, number of transferred electrons (N_e) during the dissolution and distance of transition metal and nitrogen atoms (d_{TM-N}). For comparison, standard dissolution potential (U_{diss}°) of metal atoms are also listed. Charge Transfer (Q_{TM}) on TM@TGCN systems.

Metal	E_f (eV)	U_{diss}° (V)	N_e	U_{diss} (V)	d_{TM-N} (Å)	Q_{TM} (e)
Sc	-6.17	-2.08	3	-0.02	2.05/2.09	-1.90
Ti	-5.59	-1.63	2	1.16	1.96	-1.77
V	-4.8	-1.18	2	1.22	1.94	-1.57
Cr	-2.53	-0.91	2	0.36	1.92/2.05	-1.38
Mn	-2.76	-1.19	2	0.19	2.01	-1.39
Fe	-3.15	-0.45	2	1.13	1.89	-1.08
Co	-3.32	-0.28	2	1.38	1.88	-0.93
Ni	-2.62	-0.26	2	1.05	1.96	-0.70
Cu	-1.86	0.34	2	1.27	1.89	-0.68
Zn	-0.38	-0.76	2	-0.57	2.62	-0.04
Y	-2.5	-2.37	3	-1.54	2.3	-2.52
Zr	-7.33	-1.45	4	0.38	2.09	-2.74
Nb	-6.72	-1.10	3	1.14	2.02	-2.11
Mo	-4.67	-0.2	3	1.36	1.96	-1.53
Ru	-3.21	0.46	2	2.06	1.93	-1.04
Rh	-2.71	0.60	2	1.95	2.07	-0.62
Pd	-1.43	0.95	2	1.66	2.27	-0.33
Ag	-0.64	0.95	1	1.44	2.48/2.54	-0.13
Hf	-6.76	-1.55	4	0.14	2.03	-2.43
Ta	-6.06	-0.6	3	1.42	1.99	-2.14
W	-4.81	0.1	3	1.7	1.94	-1.77
Re	-4.77	0.3	3	1.89	1.94	-1.40
Os	-4.52	0.84	8	1.41	1.93/1.97	-0.89
Ir	-2.51	1.16	3	2	2.1	-0.08
Pt	-2.5	1.18	2	2.43	1.9/3.0	-0.05

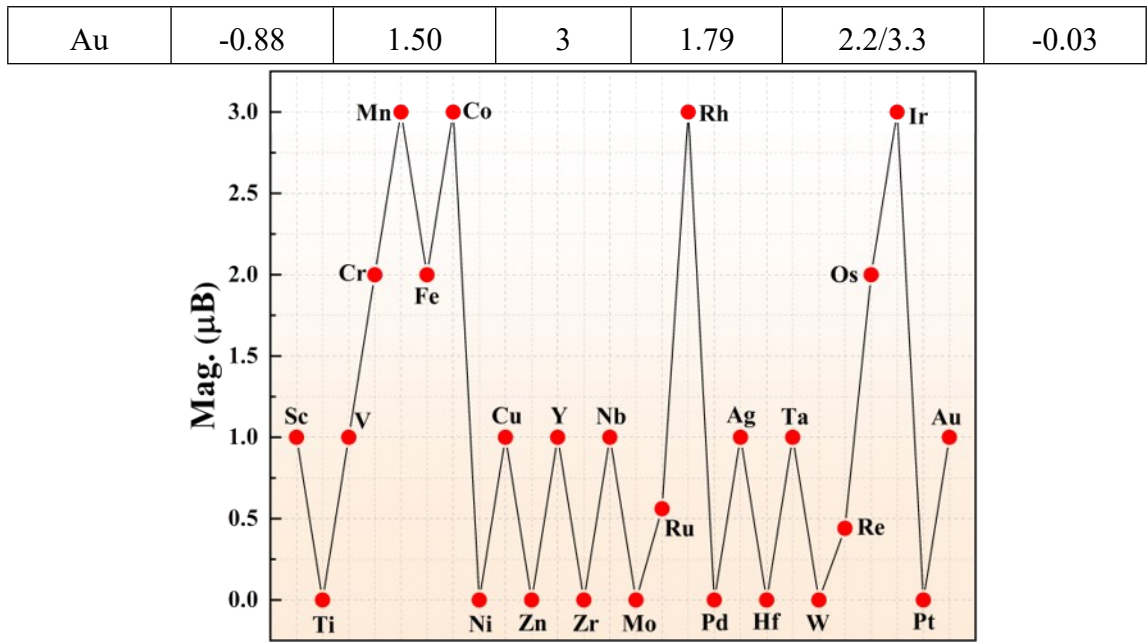


Figure S1. Total magnetic moments of TM@TGCN systems.

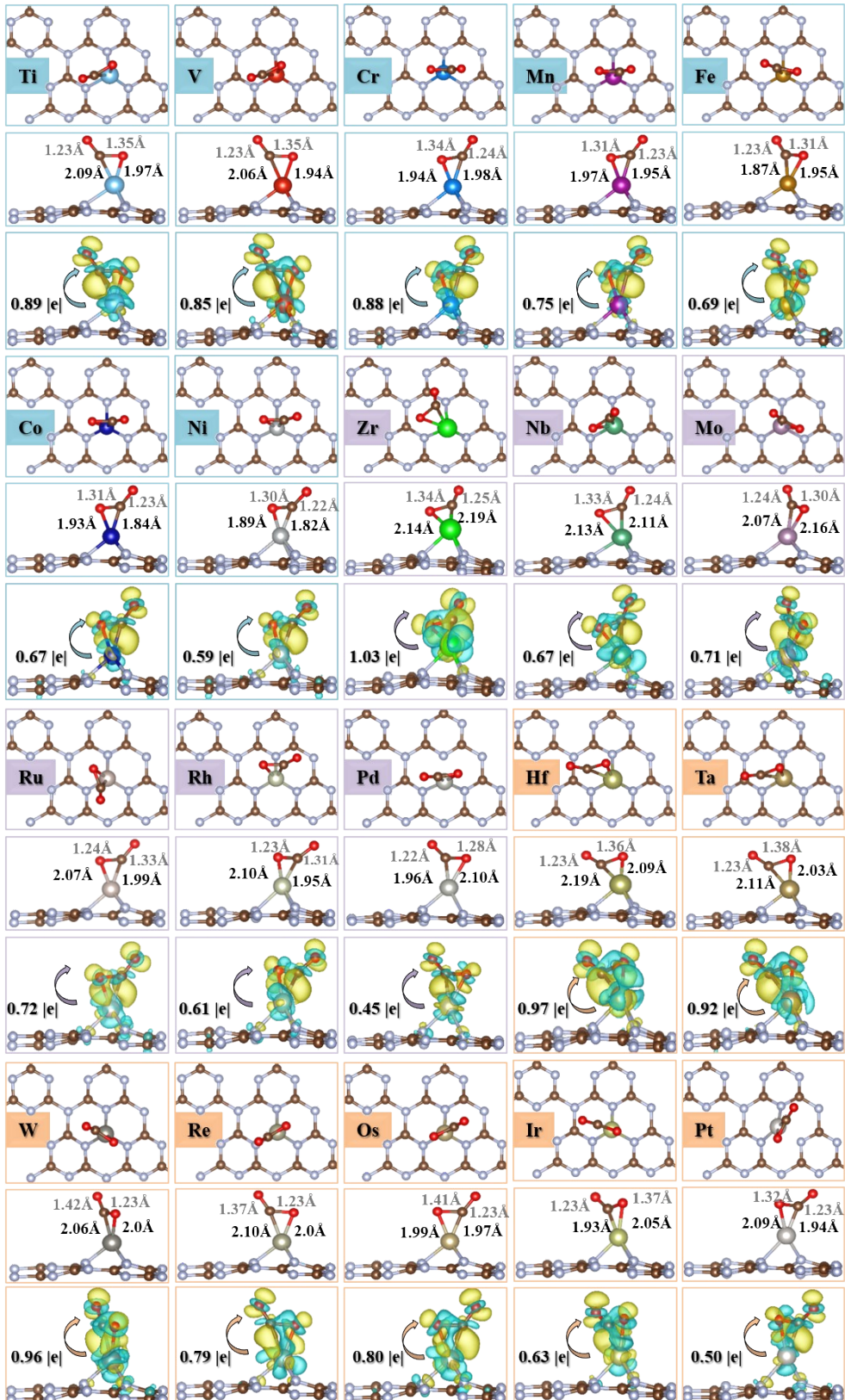


Figure S2. The most stable adsorption configuration and charge density differences of CO₂ adsorbed on TM@TGCN isosurface level is set to 0.005 e Å⁻³. Cyan and yellow area represent charge depletion and accumulation, respectively.

Table S3. The calculated Gibbs free energy changes (ΔG , eV) of the reaction intermediates in the CO₂RR and HER on the TM@TGCN monolayers.

TM@TGCN	$\Delta G[*_{CO_2}]$	$\Delta G[*_{OCHO}]$	$\Delta G[*_{COOH}]$	$\Delta G[*_H]$	$\Delta G[*_{OH}]$	$\Delta G[*_{H_2O}]$
Ti	-0.23	-0.59	0.36	0.55	-0.55	0.21
V	-0.04	-0.65	0.30	0.42	-0.59	0.09
Cr	-0.66	-0.80	-0.20	0.14	-0.96	0.01
Mn	-0.40	-0.52	0.21	-0.18	-0.07	0.72
Fe	-0.64	-0.89	-0.22	-0.32	-0.20	-0.18
Co	-0.92	-0.98	-0.20	-0.50	-0.59	-0.20
Ni	-1.86	-1.28	-0.89	-1.10	-1.24	-0.84
Cu	0.03	—	—	—	—	—
Zr	-0.88	-0.66	0.31	0.19	-1.00	0.45
Nb	-0.21	-0.56	0.40	0.41	-0.53	0.45
Mo	-0.55	-0.79	-0.24	-0.03	-0.82	-0.04
Ru	-1.46	-1.72	-0.91	-0.92	-0.96	-0.05
Rh	-1.34	-0.86	-1.22	-0.68	-0.64	-0.26
Pd	-1.01	-0.14	-0.30	-0.52	—	—
Ag	0.12	—	—	—	—	—
Hf	-0.94	-1.12	0.04	0.05	-1.21	0.20
Ta	-1.14	-1.01	-0.4	-0.19	-1.15	0.11
W	-1.05	-1.19	-0.73	-0.53	-1.43	-0.23
Re	-1.15	-1.21	-1.15	-1.02	-1.57	-0.37
Os	-2.15	-1.13	-1.49	-1.37	-1.60	0.37
Ir	-2.02	-1.45	-2.00	-1.23	-1.07	-0.80
Pt	-1.53	-0.20	-0.75	-1.07	—	—
Au	0.17	—	—	—	—	—

Scheme S1. The possible reaction pathways for CO₂RR and various products (in red) on TM@TGCN monolayers.

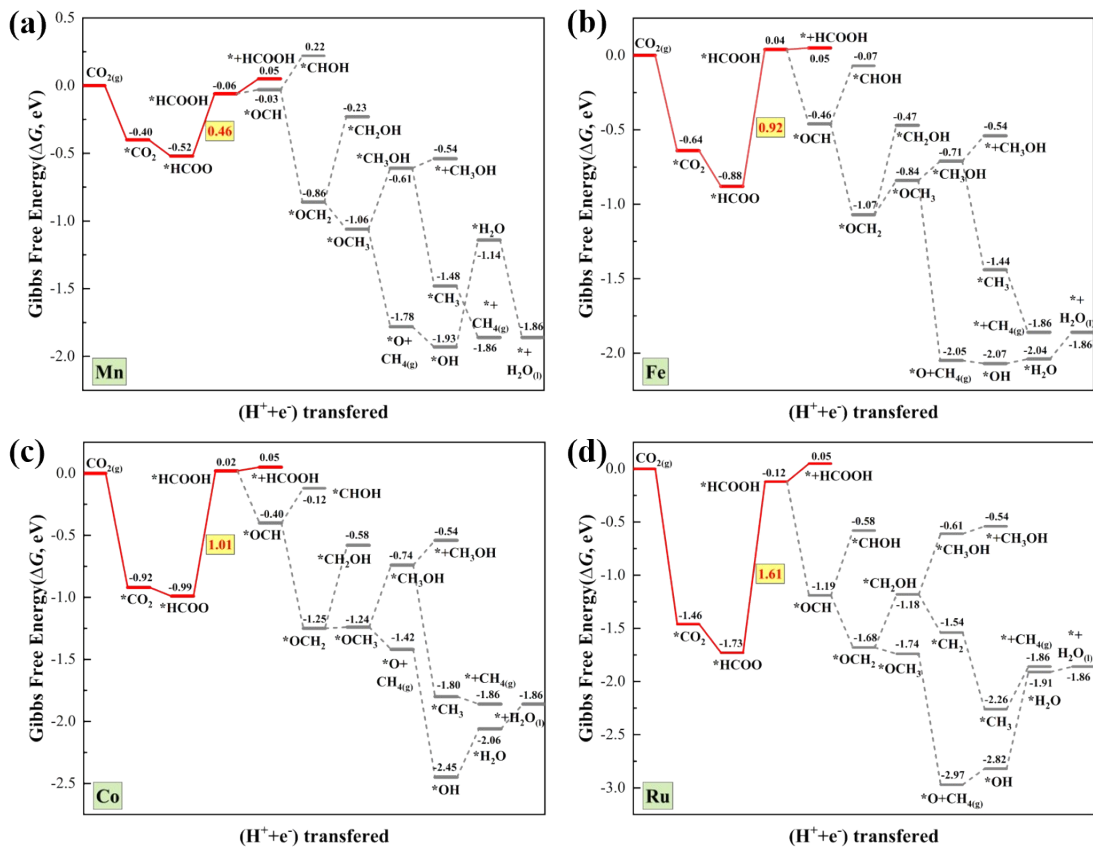
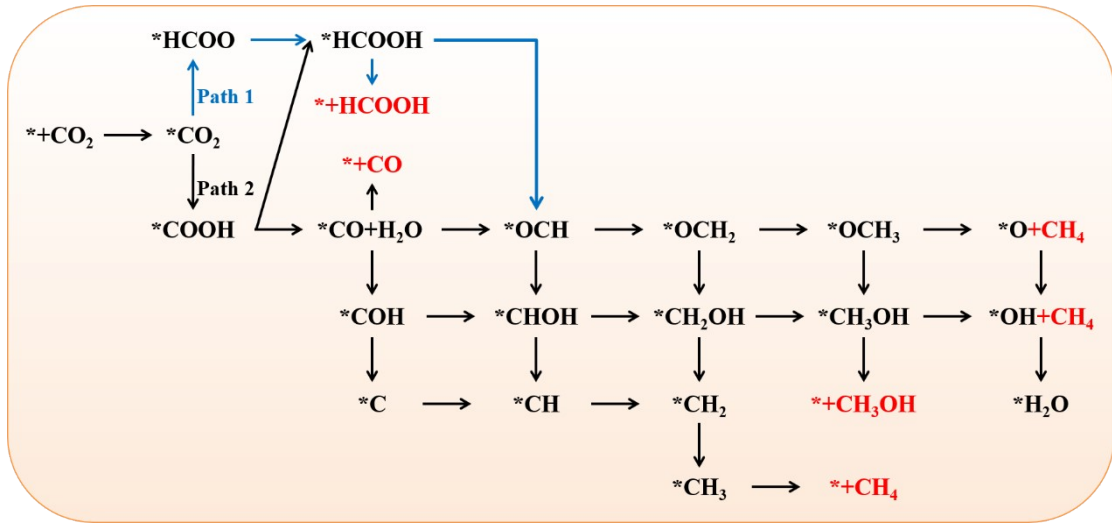


Figure S3. The Gibbs free energy diagrams of CO₂RR to C1 products on (a)

Mn@TGCN, (b) Fe@TGCN, (c) Co@TGCN and (d) Ru@TGCN at zero potential.

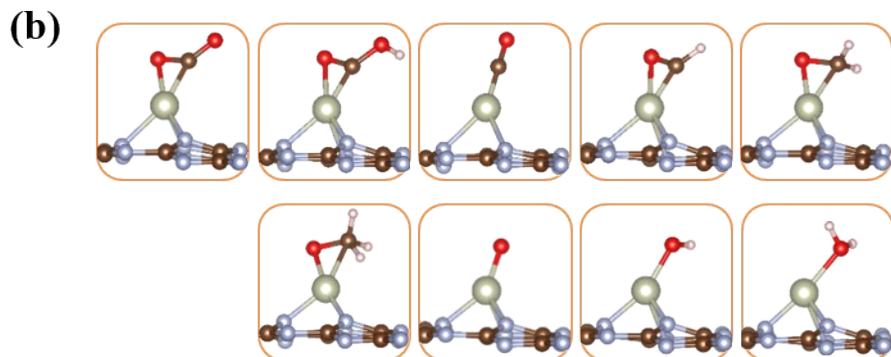
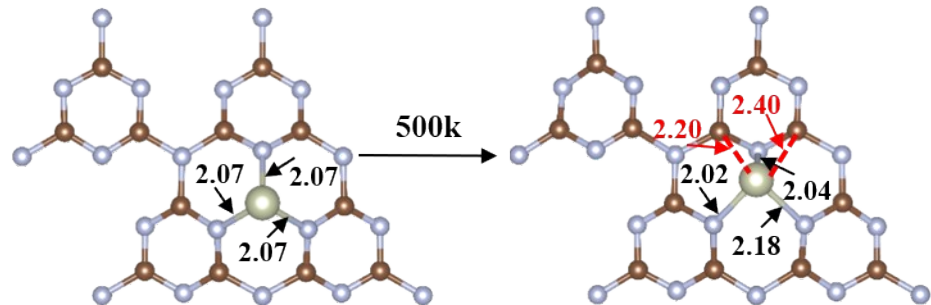
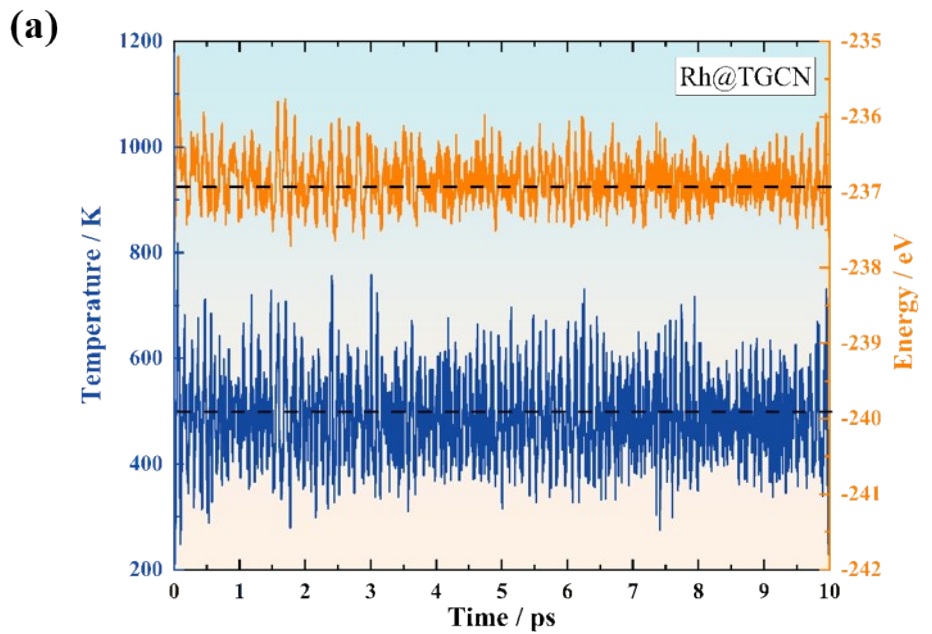


Figure S4. (a) The AIMD simulation of Rh@TGCN is run at 500 K for 10 ps with a time step of 1 fs. And top view of the final structures of Rh@TGCN monolayers after 10 ps AIMD simulations. (b) The most stable configuration of intermediates involved.

Table S4. The calculated descriptor (Φ) and d-band center on TM@TGCN based SACs.

TM@TGCN	Φ	d band center
Ti	3.50	0.82
V	4.77	0.31
Cr	6.00	-0.07
Mn	6.74	-0.35
Fe	9.38	-0.95
Co	11.13	-1.46
Ni	12.82	-1.02
Zr	2.58	1.76
Nb	4.04	1.20
Mo	6.82	-0.04
Ru	9.89	-1.48
Rh	11.86	-1.27
Pd	13.02	-1.04
Hf	2.50	0.82
Ta	3.75	0.02
W	7.34	-0.41
Re	7.07	-1.18
Os	9.51	-1.53
Ir	11.35	-1.48
Pt	12.88	-1.22

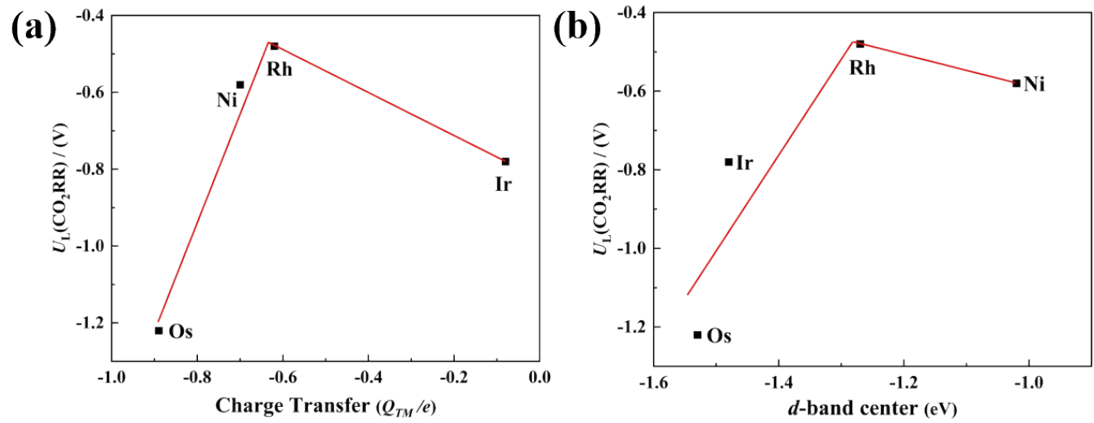


Figure S5. Volcano plot of the limiting potential of the most energy-favorable pathway for CO₂RR relative to (a) charge transfer and (b) the d-band center of (ε_d) TM@TGCN.